Available online at www.sciencedirect.com
SCIENCE DIRECT®
Materials Research Bulletin 39 (2004) 93–102
Materials Research Bulletin
www.elsevier.com/locate/matresbu

Microstructure and permittivity of sintered $BaTiO_3$: influence of particle surface chemistry in an aqueous medium

Sangkyu Lee[a], Ungyu Paik[a,*], Vincent A. Hackley[b], Yeon-Gil Jung[c], Kyung-Jin Yoon[d]

[a]*Department of Ceramic Engineering, Hanyang University, Seoul 133-791, South Korea*
[b]*Materials Science & Engineering Laboratory, National Institute of Standards and Technology, Gaithersburg, MD 20899, USA*
[c]*Department of Ceramic Science and Engineering, Changwon National University, Changwon, Kyungnam 641-773, South Korea*
[d]*Division of Chemical Metrology and Materials Evaluation, Korea Research Institute of Standards and Science, Taejon 305-600, South Korea*

Received 11 November 2002; received in revised form 18 August 2003; accepted 4 September 2003

Abstract

The influence of changes in the surface chemistry and surface composition of colloidal $BaTiO_3$, due to its dissolution and adsorption/precipitation of Ba^{2+} in an aqueous medium, on the microstructure and permittivity of sintered powder compacts was investigated. For $BaTiO_3$ powder with Ba-deficient (Ti-excess) surface prepared at pH 3, grain growth was enhanced at 1350 °C (above the eutectic) and permittivity was reduced (relative to stoichiometric $BaTiO_3$ prepared at pH 9) with increasing sintering temperature due to the liquid phase formed at grain boundaries. This same sample showed minimal grain growth and moderate enhancement of sinterability at 1300 °C (below the eutectic) attributed to sliding of the Ti-excess surface phase. $BaTiO_3$ powder treated at pH 3 and subsequently adjusted to pH 10 results in a core-shell structure with a varying near-surface stoichiometry, and produced abnormal grain growth for the compact sintered at 1350 °C. Permittivity of this sample was significantly reduced at 1350 °C due to the formation of the liquid phase, while exhibiting a similar permittivity to that of the stoichiometric sample when sintered at 1300 °C, despite significant microstructural coarsening. We conclude that changes in the surface-phase Ba/Ti ratio of particulate precursors, due to dissolution, adsorption and precipitation reactions in aqueous media, are as significant in determining the mechanical and electronic properties of the sintered material as are variations in the bulk stoichiometry of $BaTiO_3$.

Keywords: A. Ceramics; C. Electron microscopy; C. Impedance spectroscopy; D. Microstructure; D. Dielectric properties

* Corresponding author. Tel.: +82-2-2290-0502; fax: +82-2-2281-0502.
E-mail address: upaik@hanyang.ac.kr (U. Paik).

0025-5408/$ – see front matter © 2003 Elsevier Ltd. All rights reserved.
doi:10.1016/j.materresbull.2003.09.011

1. Introduction

Barium titanate ($BaTiO_3$) is a ferroelectric material used extensively in electronic applications. Its widespread application for multilayer ceramic capacitors (MLCCs) arises due to its superior dielectric properties [1]. The dielectric layers within MLCCs are formed by tape-casting of suspensions containing colloidal-sized $BaTiO_3$ particles dispersed in organic solvent- or aqueous-based media. Aqueous forming methods, though environmentally friendly and cost-effective, are more difficult to control due to reactions between the solid and liquid phases. The incongruent dissolution of $BaTiO_3$ in aqueous media at room temperature as a result of poor thermodynamic stability is well documented [2–5], and results in the leaching of Ba^{2+}. Dissolution at the $BaTiO_3$ surface in contact with water occurs according to the following reaction [3]:

$$BaTiO_3\,(s) + H_2O = Ba^{2+}\,(aq) + TiO_2\,(rutile) + 2OH^-\,(aq)$$

Under acidic conditions, the reaction can be written [4]:

$$BaTiO_3\,(s) + 2H^+\,(aq) = Ba^{2+}\,(aq) + TiO_2\,(rutile) + H_2O, \quad pK = -20.37\,(25\,^\circ C)$$

where K is the thermodynamic solubility constant. Thus, a Ba-deficient (Ti-excess) surface on $BaTiO_3$ particles is developed in acidic media. The thermodynamically predicted solubility of Ba^{2+} exceeds 1 M at pH values below about 10.2, but experimentally observed Ba^{2+} concentrations are never this high. In fact, the amount dissolved depends on both solids concentration and particle size (via specific surface area), and tends to reach a maximum at pH values below about 6. The observed solubility behavior has been explained as the result of kinetically limited diffusion through a growing surface depletion layer, with passivation by this layer [5]. The loss of Ba^{2+} from $BaTiO_3$ has also been modeled as a Langmuir surface adsorption–desorption process [6]. Both models produce a similar result, in which solubility depends (in acidic media) on the amount of available surface area per unit volume (a function of solids concentration and particle size). The kinetics of dissolution, as well as the total fraction of the $BaTiO_3$ phase depleted of Ba (on a mass basis) are profoundly enhanced when the solid phase is of colloidal dimensions [5].

The complex influence of Ba^{2+} dissolution on slip stability, sintered microstructure, and electrical properties must be thoroughly understood in order to facilitate reliable aqueous-based fabrication of $BaTiO_3$ green tape for production of MLCCs. In previous work [5,7–9], it was demonstrated that the dissolution and adsorption/precipitation behavior of Ba are critical factors in the stability of aqueous colloidal $BaTiO_3$. At acidic pH values, the formation of an oxide-rich (amorphous TiO_2) [2,10] surface phase leads to the development of a large positive surface potential at pH values below 5. It has been shown that when an acidic suspension is subsequently made basic, carbonate and/or hydroxide surface phases will appear on the $BaTiO_3$ surface as a result of the adsorption and subsequent heterogeneous precipitation of Ba^{2+} from solution [3,7,8].

This new surface phase drastically modifies the interfacial properties and surface potential of $BaTiO_3$. The dissolution and subsequent adsorption/precipitation of Ba^{2+} also create substantial problems for the control and reproducibility of dielectric properties in aqueous-based tape casting. There are a number of reports where the effects of bulk Ba/Ti ratio on sintering behavior and dielectric properties of $BaTiO_3$ have been described [11–18]. Although variations of Ba/Ti ratio within distinct surface layers on $BaTiO_3$, as a result of Ba^{2+} dissolution/precipitation, should therefore be of significant concern, this has been studied far less than the effect of bulk variations. The loss of gaseous

CO_2 (from surface carbonates) during sintering may also impede densification of $BaTiO_3$ [19]. Understanding the role of aqueous surface chemistry and surface compositional changes in the development of microstructure and permittivity is thus essential for controlling the mechanical and electrical properties of sintered $BaTiO_3$.

We present here a study that links changes in the surface composition and chemistry of $BaTiO_3$ to the microstructural development and room-temperature permittivity of sintered $BaTiO_3$ powder compacts. Stoichiometric hydrothermal $BaTiO_3$ powders were treated by controlled aqueous conditioning. In this manner, compacts were obtained having a stoichiometric Ba/Ti ratio (untreated powder), a stoichiometric core and Ti-excess surface oxide shell, or a stoichiometric core surrounded by a Ti-excess oxide inner shell and a precipitated Ba-rich outer shell. A combination of electrokinetics, electron microscopy, and impedance spectroscopy was utilized in this investigation.

2. Experimental procedure

Hydrothermal $BaTiO_3$ powder (BT-04B, Sakai Chemical Industry Co. Ltd., Japan)[1] was used in the present investigation. According to the manufacturer, this powder has a median particle size of 0.4 μm, a Ba/Ti ratio of 1.000, and a specific surface area of 3.1 ± 0.01 m^2/g. High-purity deionized water was used to prepare the $BaTiO_3$ suspension for electrokinetic analysis and aqueous conditioning, and analytical reagent grade HCl and NaOH titrants were used to adjust the suspension pH. Suspensions were prepared at a solids volume fraction of 2% for both electrokinetic sonic amplitude (ESA) measurements (ESA 8000, Matec Applied Science, Hopkinton, MA, USA) and pH conditioning. Details of the ESA method, and its application to ceramic systems, have been given previously [5]. Briefly, the dynamic electrophoretic mobility is determined from ESA measurements at a nominal frequency of 1 MHz. ESA, therefore, measures the high-frequency analog of the dc electrophoretic mobility, which depends on the electrical potential existing at the solid–liquid interface. The suspension pH was pre-adjusted considering the aging effect, with a target of pH 3 or 9 after aging for 12 h. In a second experiment, a suspension that had first been conditioned at pH 3 for 12 h, was subsequently readjusted to pH 10 (henceforth referred to simply as the pH 10 sample). We performed this basic pH adjustment in order to form a Ba carbonate/hydroxide phase on the previously Ba-depleted surface. After conditioning, samples were centrifuged at 15,000 rpm (J2-21 Beckman, USA) for 30 min. The resulting sediment was air dried for 24 h and then granulated with the addition of poly(vinyl alcohol) (PVA) as a binder.

Green compacts were uniaxially formed from granulated powders at 5 MPa and then hydrostatically pressed under 100 MPa. The pressed pellets were sintered at 1250, 1300, and 1350 °C at a 5 °C/min ramp in ambient atmosphere, after which they were quenched to room temperature. At 1350 °C, sintering was carried out with and without a dwell time of 2 h. The microstructure of the sintered specimens was observed by scanning electron microscope (SEM, Hitachi, Model S-4200, Japan). For SEM, depending on whether a liquid phase had formed, samples were imaged either at the fracture surface or at the polished and chemical etched (using a mixture of H_2SO_4, NHO_3, and HF) surface.

[1] Certain trade names and company products are mentioned in the text or identified in illustrations in order to specify adequately the experimental procedure and equipment used. In no case does such identification imply recommendation or endorsement by National Institute of Standards and Technology, nor does it imply that the products are necessarily the best available for the purpose.

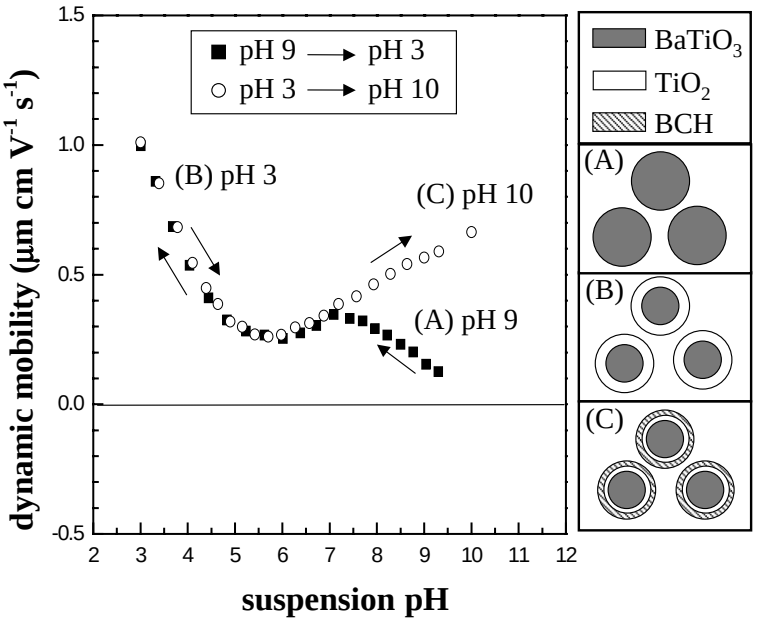

Fig. 1. Electrokinetic behavior of colloidal $BaTiO_3$ (in 0.01 M $NaNO_3$ aqueous solution) and schematic illustration of changes in the surface composition (insets A–C) with suspension pH.

For permittivity measurements, the pressed pellets were sintered at 1300 and 1350 °C for 2 h at a 5 °C/min ramp in an ambient atmosphere. The room-temperature permittivity was measured at 1 kHz with an impedance analyzer (Model HP4192, Hewlett-Packard, Tokyo, Japan).

3. Results and discussion

The relationship between surface composition and electrokinetic behavior (i.e. dynamic mobility) of $BaTiO_3$ particles is illustrated in Fig. 1.[2] The particles depicted in Fig. 1 (inset (A)), represent the native, unmodified (stoichiometric) $BaTiO_3$. Dynamic mobility data indicate an isoelectric point (pH_{IEP}) for this material that is fairly basic (near pH 10). In general, the pH_{IEP} represents the point of least solubility, so these powders should be relatively stable toward dissolution and thus maintain their initial composition when treated in an aqueous solution at pH 9. As the suspension pH decreases below pH 7 and approaches pH 3, dissolution of Ba from the surface region leaves an oxide-rich layer as depicted in Fig. 1 (inset (B)). The development of this oxide layer corresponds to an initially decreasing, then sharply increasing positive dynamic mobility. The low-pH portion of the electrokinetic curve (represented by filled symbols

[2] Surface potential cannot be measured directly, and surface charge determination requires extensive pH titrations that would not be possible in a thermodynamically unstable system such as this. Therefore, electrokinetic measurements are commonly utilized, from which surface charge behavior is inferred. Electrokinetic measurements are also a better predictor of colloidal stability, since they reflect the zeta potential at the plane of shear, and include the effects of ionic screening and specific adsorption.

in Fig. 1) is characteristic of a TiO_2-like charged surface [5]. As a result of the reverse sequence from pH 3 to 10, the electrokinetic curve deviates positively from the acid titration curve at pH values above about 7.

This increase in the dynamic mobility above pH 7 indicates a more basic, and fundamentally different surface from the native $BaTiO_3$ that existed prior to acid-base conditioning. Thus, hysteresis in the dynamic mobility curve results from changes in the electrochemical properties of the interface, and is indicative in this case of a new surface phase. In effect, a three-phase composite particle is created by the acid–base treatment as depicted in Fig. 1 (inset (C)), with a $BaTiO_3$ core surrounded by an Ti-excess layer surrounded by a precipitated Ba-rich phase. Thermodynamic considerations [4] and previous XPS results [8] indicate that the precipitate phase in this case likely consists of $BaCO_3$ and/or $Ba(OH)_2$. It has not been possible to resolve the surface composition or precipitation reaction further, since CO_2 is ubiquitous and carbonates are always detected on $BaTiO_3$ surfaces, and can easily result from sample preparation artifacts prior to analysis. Therefore, the carbonate surface phase could form during pH conditioning or it might form during the subsequent drying step when the particles come in contact with CO_2 in the atmosphere, or both.

SEM images in Fig. 2 show microstructure as a function of both sintering temperature (below the eutectic temperature) and aqueous conditioning of the starting powders. The grains of compacts

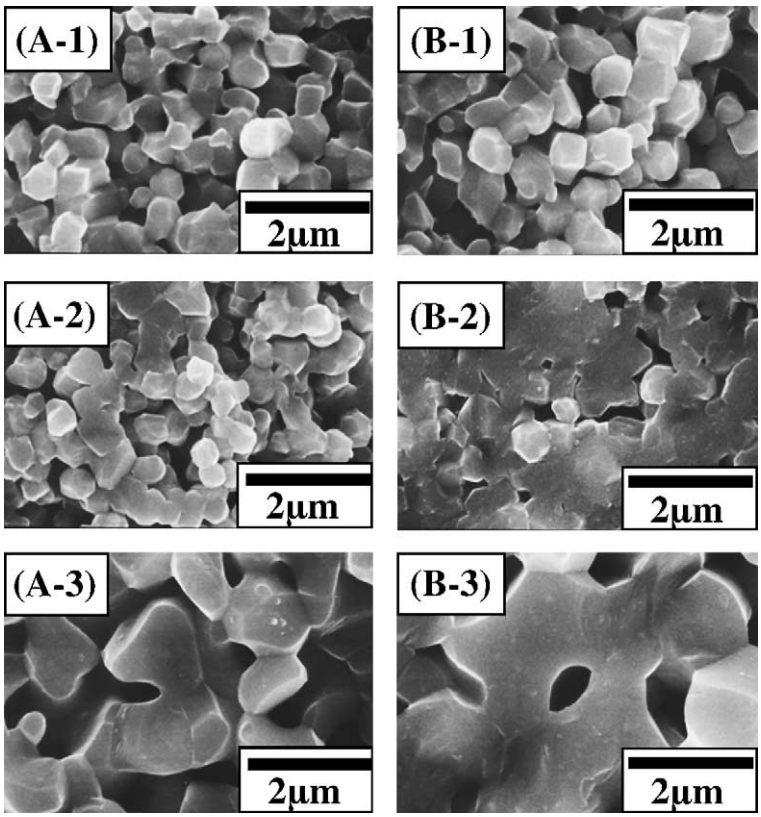

Fig. 2. Microstructure in fracture surfaces of $BaTiO_3$ compacts sintered at (A) 1250 °C and (B) 1300 °C without dwell time for each pH conditioning treatment. The micrographs marked 1, 2, and 3 indicate specimens prepared from powders conditioned at pH 9, 3, and 3–10, respectively.

sintered at 1250 °C and pre-conditioned at pH 9 (Fig. 2(A-1)) and pH 3 (Fig. 2(A-2)) maintained a size that is close to the initial particle size of the starting powder (i.e. about 0.4 μm). A significant amount of necking is apparent between grains, independent of the conditioning pH, an indication of the initial sintering stage. For the pH 10 conditioned sample, coarsening is significantly enhanced, yielding a grain size of about 1 μm (Fig. 2(A-3)). For compacts sintered at 1300 °C, densification proceeded with or without grain growth, for powders conditioned at pH 10 and 3, respectively. Whereas, compacts conditioned at pH 9 showed a microstructure similar to that obtained at the lower temperature (1250 °C), with a slight increase in the average grain size (Fig. 2(B-1)).

It has been proposed by Abicht and co-workers [10,20] that the amorphous TiO_2 surface phase formed on acid-conditioned $BaTiO_3$ promotes densification below the eutectic temperature of the pseudo-binary $BaTiO_3$–$Ba_6Ti_{17}O_{40}$ system (1332 °C) [21], by facilitating the sliding of individual $BaTiO_3$ grains. Another possibility to enhance densification is impurities in the starting materials, which could decrease the liquid formation temperature [22]; the same starting powder was used for all experiments in the present study and only high purity chemicals (acid, base) and deionized water were employed, which should rule out impurities in explaining observed differences between the powders treated under different pH conditions. Densification (based on the elimination of pores) at 1300 °C for the powder conditioned at pH 3 is attributed to the enhanced sliding effect, as this sample conforms to the simple core-shell structure discussed by Abicht and co-workers [10,20]. The pronounced grain growth and densification exhibited by the sample conditioned at pH 10 must be attributed to the presence of the Ba-rich outer shell and/or the multi-shell structure itself, since the overall Ba/Ti ratio is probably close to stoichiometric (i.e. the Ba initially leached from the inner oxide shell during acid conditioning is subsequently redeposited in the outer carbonate/hydroxide shell at pH 10, thus preserving the original Ba/Ti ratio of the untreated material).

Given that the second decomposition step for $BaCO_3$ occurs near 1300 °C, in a reaction with $BaTiO_3$ to form Ba_2TiO_4 and CO_2 [19], this reaction could also contribute to the formation of the coarsened microstructure observed in the pH 10 sample. However, the first $BaCO_3$ decomposition, which occurs between 500 and 900 °C to form $BaTiO_3$ by the reaction with TiO_2 in the surface layer, has been attributed to surficial carbonate that is easily removed by acid washing [19]. Since open porosity is still present at this stage, the low temperature reaction does not impact microstructure. The high temperature decomposition reaction was attributed to a more stable form of carbonate, possibly existing in the bulk phase as a result of incomplete conversion of $BaCO_3$ during synthesis [23]. If this is correct, then the presumed surface precipitated carbonate on the pH 10 sample should decompose during the first (low temperature) step, and not at 1300 °C. Effects of $BaCO_3$ decomposition during sintering of $BaTiO_3$, synthesized by solid-state reaction of $BaCO_3$ and TiO_2 powders, have been reported previously [19,24,25].

Increasing the sintering temperature above the eutectic to 1350 °C produces a profound effect on the microstructure due to the formation of the liquid phase. For the stoichiometric $BaTiO_3$ conditioned at pH 9, the grain size was increased to about 1 μm and densification progressed (Fig. 3(A-1)). After a 2-h dwell time, grain growth was noticeably manifested due to the formation of the liquid phase and residual pores were intra-granularly located as shown in Fig. 3(B-1). In this case, the grain size was about 20 times (≈8 μm) larger than the starting particle size (≈0.4 μm). The pH 3 conditioned sample sintered at 1350 °C exhibited severe grain growth with a grain size of approximately 30 μm as shown in Fig. 3(A-2). However, the liquid-phase induced abnormal grain growth was not observed in this case, a result that is inconsistent with previous reports [18,19] that associated abnormal grain growth with

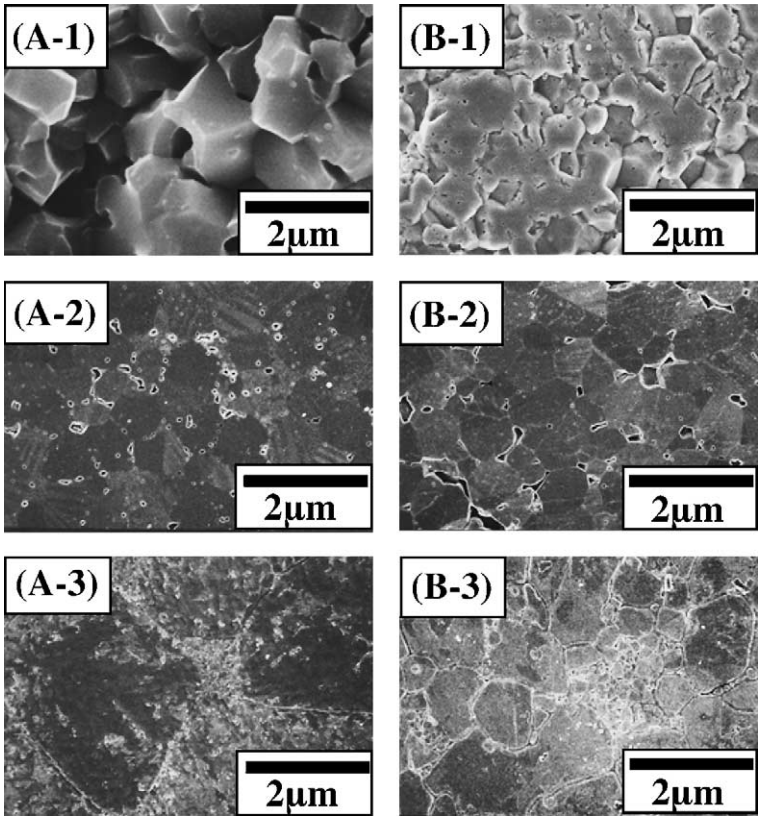

Fig. 3. Microstructure in the polished and chemically etched surface of $BaTiO_3$ compacts sintered at 1350 °C for each pH conditioning treatment: (A) without, and (B) with 2-h dwell time applied at the sintering temperature. The micrographs marked 1, 2, and 3 indicate specimens prepared from powders conditioned at pH 9, 3, and 3–10, respectively; (A-1) is imaged in the fracture surface.

Ti-excess. No further significant microstructural development occurred in the specimen after a 2-h dwell time, except an increase in the liquid phase content.

The compact sintered at 1350 °C and derived from the pH 10 treated powder, shown in Fig. 3(A-3), indicates a microstructure consisting of small matrix grains ~2 μm in size, surrounding abnormally large grains of about 100 μm. After a dwell time of 2 h at 1350 °C (Fig. 3(B-3)) the fine matrix grains were replaced by a new set of abnormally grown coarse grains with sizes exceeding 100 μm, and by a fairly broad range of smaller sized grains (<20 μm). The abnormal grain growth exhibited by the pH 10 sample must therefore be attributed to the heterogeneous adsorption/precipitation of Ba^{2+} onto the Ti-excess particle surface, indicating that local nanoscale variations in the Ba/Ti ratio and phase composition are at least as important for microstructural development as the bulk Ba/Ti ratio.

Fig. 4 shows the variation of room-temperature permittivity as a function of conditioning pH and sintering temperature. The permittivity decreases with an increase in sintering temperature above the eutectic temperature, independent of the particle surface treatment. The sample conditioned at pH 9 retains a relatively high permittivity, even at the higher sintering temperature, compared to powders treated in acidic suspensions. The sample conditioned at pH 3 indicates a low permittivity at both

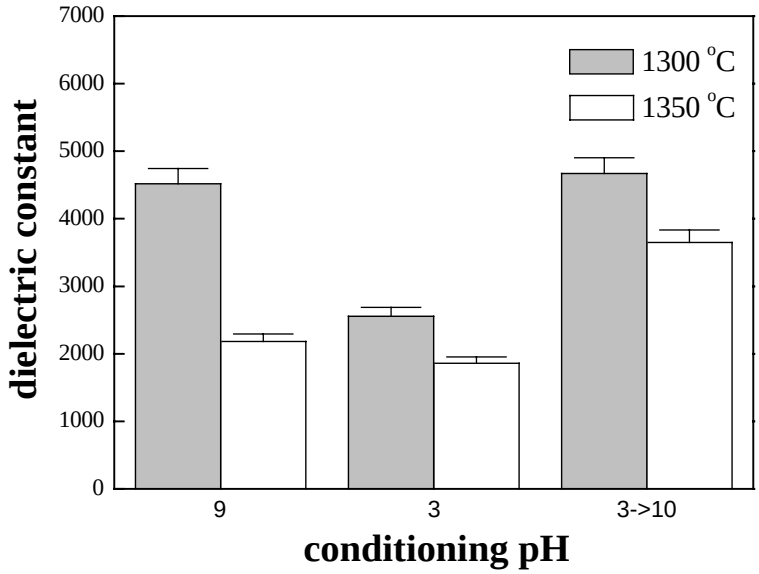

Fig. 4. Variation of room temperature dielectric permittivity as a function of conditioning pH and sintering temperature.

sintering temperatures (1300 and 1350 °C). However, the high permittivity at 1300 °C for the pH 10 sample, which is similar in magnitude to the sample treated at pH 9, drastically decreases with an increase to 1350 °C. Overall, there does not appear to be a direct correlation between grain growth and permittivity for samples sintered at the lowest sintering temperature.

Generally speaking, for stoichiometric $BaTiO_3$, permittivity should scale inversely with grain size and proportionally with sintered density [26–28]. However, Lee et al. [15] report that density and grain size are not the dominant factors determining the permittivity of sintered $BaTiO_3$ with nonstoichiometric compositions. They attributed the low permittivity observed in Ti-excess $BaTiO_3$ to the presence of a continuous Ti-excess grain boundary phase within which the $BaTiO_3$ grains are embedded; according to a model developed by Chen et al. [29], the permittivity in such a system decreases with an increase in the width of the grain boundary phase. However, Lee et al. [15] who sintered at 1350 °C, base their explanation on the formation of a eutectic melt, from which the Ti-excess grain boundary phase solidifies during cooling.

In the present work, the Ti-excess (i.e. pH 3 conditioned) sample exhibited the lowest permittivity at both sintering temperatures. The low permittivity for the pH 3 sample at 1300 °C is attributed to the low Ba/Ti ratio. At 1350 °C, the permittivity is reduced for all three samples, most likely due to the formation of a liquid phase above the eutectic point. Here, grain size is implicated as a factor leading to the reduced permittivity. The large relative decrease in permittivity for the pH 10 conditioned sample upon increasing the sintering temperature can further be attributed to abnormal grain growth. The two nonstoichiometric samples (powders conditioned at pH 3 and 3 followed by pH 10) produce the largest grain growth and lowest permittivities. In both cases, nonstoichiometry exists primarily at a local level, within shell layers and at the interfaces between the core and shell layers.

A Ba-rich surface layer can be formed on $BaTiO_3$, in particular a leached $BaTiO_3$ surface, during aging of a suspension because suspension pH spontaneously increases until equilibrium is reached. Passivation mechanisms to prevent Ba^{2+} leaching and subsequent adsorption/precipitation of Ba^{2+}

during the aqueous forming process, must be developed in order to resolve the substantial problems associated with the core-shell structures postulated here. These structures can lead to reduced permittivity and grain coarsening, and, in the latter case, to abnormal grain growth.

4. Conclusions

The overall Ba/Ti ratio (stoichiometry) is important for determining permittivity of sintered $BaTiO_3$, but also the local compositional distribution appeared critical. The surface composition of $BaTiO_3$ powders was modified during wet processing by the dissolution and precipitation of Ba^{2+} during conditioning at pH 3 and at pH 10 (after initial treatment at pH 3). These surface effects can lead to adverse changes in microstructure development and permittivity similar to those attributed to bulk nonstoichiometries in the starting powder. At low sintering temperature (below the eutectic point), the Ba/Ti ratio of the powder seemed to be key in determining permittivity, with Ti-excess (i.e. conditioned at pH 3) leading to a decreased permittivity. At high sintering temperature (above the eutectic), an apparent correlation existed between liquid phase formation and decreased permittivity, with local variations in stoichiometry having a huge impact on grain growth. A multi-shell-structured powder (produced by conditioning first at pH 3 followed by adjustment to pH 10), with a Ba/Ti ratio that varies across the grain interface (from <1 to >1 to 1), produced abnormal grain growth and low permittivity with an increase of sintering temperature to 1350 °C. Here, the nanoscale variations in stoichiometry appeared to be critical. For the pH 10 conditioned sample, the second decomposition reaction for $BaCO_3$ and the heterogeneous adsorption/precipitation of dissolved Ba^{2+} were suspected as contributing to the grain growth at low sintering temperature (1300 °C) and the abnormal grain growth at high sintering temperature (1350 °C), respectively. However, a clear picture of the underlying sintering mechanism has yet to emerge. The ''stoichiometric'' powder (conditioned at pH 9) exhibited the highest permittivities and the most uniform microstructures over the temperature range from 1300 to 1350 °C. In contrast to previous reports regarding bulk Ti-excess powders, the surficially Ti-excess hydrothermal powder (i.e. the sample treated at pH 3) did not exhibit abnormal grain growth, despite the observed reduction in permittivity.

Acknowledgements

This work was financially supported by the Korea Institute of Science and Technology Evaluation and Planning (KISTEP) through the 21 Century Frontier Projects.

References

[1] J. Nowotny, M. Rekas, Electronic Ceramic Materials, in: J. Nowotny (Ed.), Trans Tech, Zürich, Switzerland, 1992.
[2] D.A. Anderson, J.H. Adair, D. Miller, J.V. Biggers, T.R. Shrout, Surface chemistry effects on ceramic processing of $BaTiO_3$ powder, in: G.L. Messing, E.R. Fuller, Jr., H. Hausner (Eds.), Ceramic Powder Science II, Ceramic Transactions, vol. 1, American Ceramic Society, Westerville, OH, 1988, pp. 485–492.
[3] M.C. Blanco López, B. Rand, F.L. Riley, J. Euro. Ceram. Soc. 17 (1997) 281–287.
[4] S. Venigalla, J.H. Adair, Chem. Mater. 11 (1999) 589–599.

[5] U. Paik, V.A. Hackley, Influence of solids concentration on the isoelectric point of aqueous barium titanate, J. Am. Ceram. Soc. 83 (2000) 2381–2384.
[6] A. Neubrand, R. Lindner, P. Hoffmann, J. Am. Ceram. Soc. 83 (2000) 860–864.
[7] X.Y. Wang, S.W. Lu, B.I. Lee, L.A. Mann, Mater. Res. Bull. 35 (2000) 2555–2563.
[8] U. Paik, J.G. Yeo, M.H. Lee, V.A. Hackley, Y.-G. Jung, Mater. Res. Bul. 37 (2002) 1623–1631.
[9] S. Lee, V.A. Hackley, U. Paik, Influence of barium dissolution on the electrokinetic properties of colloidal $BaTiO_3$ in an aqueous medium, J. Am. Ceram. Soc. 86 (2003) 1662–1668.
[10] H.-P. Abicht, D. Völtzke, R. Schneider, J. Woltersdorf, O. Lichtenberger, Mater. Chem. Phys. 55 (1998) 188–192.
[11] T. Lin, C. Chu, J. Am. Ceram. Soc. 73 (1990) 531–536.
[12] P.P. Phule, S.H. Risbud, J. Mater. Sci. 25 (1990) 1169–1183.
[13] A. Beauger, J.C. Mutin, J.C. Niepce, J. Mater. Sci. 19 (1984) 195–201.
[14] Y.H. Hu, M.P. Harmer, D.M. Smith, J. Am. Ceram. Soc. 68 (1985) 372–376.
[15] J.K. Lee, K.S. Hong, J.W. Jang, J. Am. Ceram. Soc. 84 (2001) 2001–2006.
[16] C. Hérard, A. Raivre, J. Lemaître, J. Euro. Ceram. Soc. 15 (1995) 145–153.
[17] S. Venigalla, J.H. Adair, Chem. Mater. 11 (1999) 589–599.
[18] K.W. Kirby, B.A. Wechsler, J. Am. Ceram. Soc. 74 (1991) 841–847.
[19] C. Hérard, A. Raivre, J. Lemaître, J. Euro. Ceram. Soc. 15 (1995) 145–153.
[20] D. Völtzke, H.P. Abicht, J. Woltersdorf, E. Pippel, Mater. Chem. Phys. 73 (2002) 274–280.
[21] K.W. Kirby, B.A. Wechsler, J. Am. Ceram. Soc. 74 (1991) 841–847.
[22] M.H. Lin, J.F. Chou, H.Y. Lu, J. Euro. Ceram. Soc. 20 (2000) 517–526.
[23] M.C. Blanco López, G.. Fourlaris, B. Rand, F.L. Riley, J. Am. Ceram. Soc. 82 (1999) 1777–1786.
[24] T.J. Carbone, J.S. Reed, Ceramic Bull. 58 (1979) 512–515.
[25] A. Beauger, J.C. Mutin, J.C. Niepce, J. Mater. Sci. 18 (1983) 3543–3550.
[26] G. Arlt, D. Hennings, G. de With, J. Appl. Phys. 58 (1985) 1619–1625.
[27] M.H. Fery, D.A. Payne, Phys. Rev. 54 (1996) 3156–3158.
[28] W.R. Buessem, L.E. Cross, A.K. Goswami, J. Am. Ceram. Soc. 49 (1966) 33–36.
[29] J. Chen, A. Grton, H.M. Chan, M.P. Harmer, J. Am. Ceram. Soc. 69 (1986) C303–C305.